Buffer-aided max-link relay selection in amplify-and-forward cooperative networks

http://dx.doi.org/10.1109/TVT.2014.2324761

PUBLISHER

© IEEE

VERSION

AM (Accepted Manuscript)

On the Study of max-link Relay Selection in Amplify-and-Forward Cooperative Networks

Zhao Tian, *Student Member, IEEE*, Gaojie Chen, Yu Gong, Zhi Chen, *Member, IEEE* and Jonathon Chambers, *Fellow, IEEE*

Abstract

This paper investigates the outage performance of the amplify-and-forward (AF) relay system which exploits buffer-aided max-link relay selection. Both the asymmetric and symmetric source-to-relay and relay-to-destination channel configurations are considered. We successfully derive the closed-form expression for the outage probability, and analyze the average packet delay. We prove that the diversity order is between N and $2N$ (where N is the relay number), corresponding to a relay buffer size between 1 and ∞ respectively. We also analytically show the coding gain. Numerical results are given to verify the analysis in this paper.

Index Terms

Cooperative networks, relay selection, amplify-and-forward (AF)

I. Introduction

Relay selection can be applied in either a non-regenerative (e.g. amplify-and-forward (AF)) or a regenerative (e.g. decode-and-forward (DF)) relay systems [1]. The *max-min* relay selection is often considered as an optimum DF relay selection scheme, in which the best relay is selected with the highest gain among all of the minimum of the source-to-relay and relay-to-destination channel gain pairs [2]. Although the *max-min* schemes achieves diversity order of N (where N is the number of available relays), its performance is practically limited by the constraint that the best source-to-relay and relay-to-destination links for a packet transmission must be determined concurrently. Recent research has on the

Z. Tian, G. J. Chen, Y. Gong and J. Chambers are with the Advanced Signal Processing Group, Loughborough University, Loughborough, Leicestershire, UK, Emails: { z.tian,g.chen,y.gong,j.a.chambers }@lboro.ac.uk.

Z. Chen is with the National Key Laboratory of Science and Technology on Communications, University of Electronic Science and Technology of China, Chengdu, Sichuan 611731, China, E-mail: chenzhi@uestc.edu.cn.

other hand found that, by introducing data buffers at the relays, this constraint can be relaxed to yield significant performance advantage in practical systems [3]–[8].

An early example of buffer-aided relay selection is the *max-max* scheme [6]. In the max-max relay selection, at one time slot t, the best link among all source-to-relay channels is selected, and a data packet is sent to the selected relay and stored in the buffer. At the next time slot $t+1$, the best link among all relay-to-destination channels is selected, and the selected relay (which is often not the same relay selected at time t) forwards one data packet from its buffer to the destination. In this way, the strongest links from both source-to-relay and relay-to-destination group channels are always selected so that it has significant coding gain over the traditionary *max-min* scheme.

The *max-max* relay selection still follows the traditional transmission order then the source-to-relay and relay-to-destination transmissions always carry on in an alternative manner, with a diversity order of N which is the same as that for the *max-min* scheme. In the recent *max-link* approach [4], [8], this constraint on the transmission order is further relaxed so that, at any time, a best link is selected among all available source-to-relay and relay-to-destination links. Depending on whether a source-to-relay or a relay-to-destination link is selected, either the source transmits a packet to the selected relay or the selected relay forwards a stored packet to the destination. It is shown in [4] that the *max-link* relay selection not only has coding gain over the *max-min* scheme, but also has higher diversity order than both the *max-min* and *max-max* schemes. In particular, the diversity order can approach $2N$ when the relay buffer size is large enough.

While the buffer-aided relay selection describes a promising way in the cooperative networks, existing approaches has been mainly for the DF relay systems (e.g. [3]–[8]). This naturally arises the following two questions:

- *Whether is it necessary or not to apply buffer-aided relay selection in the AF relay network?* In the AF system, the relay simply amplifies and forwards the received signal to the destination. Because the AF does not decode the received packets, it not only is easier to implement but also has higher level of security than the DF system. When the data buffers are applied at the relays, another difference between the DF and AF is that they need to store "decoded digital data" and "received real signal" in the buffers respectively. This brings up two implementation issues: quantization and data storage. It is interesting to point out that, because the relay works in the half-duplex mode that it receives a data packet at one time slot and forwards it out at another slot, a data buffer (of size 1) actually exists even in the traditional AF or DF relay system. In order to store the data in the buffer, the quantization is always necessary for both AF and DF systems, no matter whether the buffers are used or not. Compared to its DF counterpart, therefore, the buffer-aided AF relay selection has the extra implementation cost of storing quantized "real signal", but it retains the advantage of no decoding at the relays, making it particularly attractive in many applications such as the mobile relays which are not always allowed to decode the source messages.

- *How is the buffer-aided relay selection applied in the AF cooperative networks?* In the traditional AF relay selection, the best relay is selected with the highest end-to-end signal-to-noise-ratio (SNR) at the destination [9], which is termed as the AF *max-SNR* scheme in this paper. When the AF relays are equipped with data buffers, however, the traditional max-SNR or its variants (e.g. [10]–[12]) cannot be used. This is because now the source-to-relay and relay-to-destination links are selected separately and then the end-to-end SNR at the destination cannot be obtained instantaneously. In this paper, following the traditional relay selection that the DF relay selection schemes such as the max-min may also be applied in the AF system (e.g. [13]), we propose to apply the DF max-link in the AF buffer-aided relay selection.

Of particular importance is the outage probability of the buffer-aided AF relay selection system. In the DF system, generally, the outage probability for the source-to-relay and relay-to-destination transmission can be obtained separately and then combined to the give the overall outage probability. In contrast, the outage performance of an AF relay system depends on the probability distribution of the end-to-end SNR at the destination, making it usually harder to analyze than that of its DF counterpart. Particularly, when the relay buffer is introduced in the AF relays, the best source-to-relay and relay-to-destination links for a packet transmission are determined at different times, thus they may be selected from different numbers of available links. As a result, the distribution of the end-to-end SNR no longer follows the form of the MacDonald distribution as that in the traditional AF *max-SNR* relay selection [9]. This makes the outage performance of the buffer-aided AF relay selection much more difficult to analyze than both the traditional max-SNR scheme and the buffer-aided DF max-link scheme. This is perhaps the main reason that the AF buffer-aided relay selection has not been well studied.

In this paper, the buffer-aided AF max-link relay selection is carefully investigated. Unlike existing buffer-aided relay selection approaches (e.g. [3], [5], [7]), this paper considers an asymmetric channel configuration that the average gains for the source-to-relay and relay-to-destination channels are not the same. While the asymmetric channel assumption makes the analysis even more difficult, it represents a more practical scenario so that the analysis provides an important basis for new system design. The main contributions of this paper is summarized as follows:

- Analyzing the outage probability of the AF max-link scheme for both the asymmetric and symmetric channel configuration. As far as we know, this is the first time to consider asymmetric channels in buffer-aided relay selection, and also the first to derive the outage probability closed-form for the AF buffer-aided relay selection scheme. Numerical simulation is given to verified the analysis. The results show that the outage performance gain of the AF max-link scheme over the traditional max-SNR scheme is more significant in the symmetric than in the asymmetric channels. This gives an important insight in designing the buffer-aided relay systems: for example, power controls at the source and relay nodes may be used to achieve symmetric channel configuration for better outage performance.
- Analyzing the average packet delays for both the asymmetric and symmetric channels. The results show that, when the relay-to-destination channels are stronger than the source-to-relay channels, the AF buffer-aided relay system has the shorter delay. Therefore, the "best" delay and outage performance requires different channel conditions. This actually brings up an interesting design topic for future study: how the delay and outage performance can be well balanced.
- Proving that the diversity order of the AF max-link relay selection is between N and $2N$ (where N is the number of relays), and the lower and upper diversity limits are reached when the relay buffer size L is 1 and ∞ respectively.
- Analytically showing the coding gain of the AF max-link scheme compared to the traditional AF max-SNR schemes.

The rest of the paper is organized as follows: Section II describes the buffer-aided AF max-link relay selection; Section III derives the closed-form expression of the outage probability; Section IV analyzes the average packet delay; Section V studies the diversity order; Section VI shows the coding gain; Section VII shows numerical simulations to verify the analysis; finally Section VIII summarizes the paper.

II. AF MAX-LINK RELAY SELECTION

The system model of the buffer-aided AF relay selection is shown in Fig. 1, where there is one source node (S), one destination node (D) and N relay nodes (R_k, $1 \leq k \leq N$). All nodes operate in the half-duplex mode, that is they do not transmit and receive simultaneously. Each relay is equipped with a data buffer Q_k $(1 \leq k \leq N)$ of finite size L (in the number of data packets). The data packets in the buffer obey the "first-in-first-out" rule.

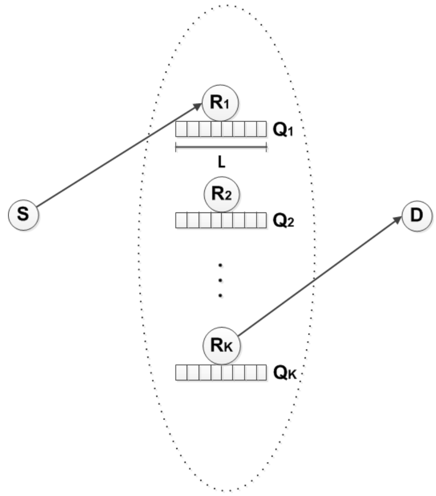

Fig. 1. The system model of the buffer-aided AF relay selection.

In this paper, we assume no direct transmission link between the source and destination nodes[1]. We denote $h_{SR_k}(t)$ and $h_{R_kD}(t)$ as the channel coefficients for $S \rightarrow R_k$ and $R_k \rightarrow D$ at time slot t respectively. We assume the all channel coefficients are independently and slowly Rayleigh fading such that they remain unchanged during one packet duration but independently vary from one packet time to another. The average $S \rightarrow R_k$ and $R_k \rightarrow D$ channel gains are assumed as

$$\mathrm{E}[|h_{SR_k}(t)|^2] = \sigma^2_{h_{sr}} \qquad \mathrm{E}[|h_{R_kD}(t)|^2] = \sigma^2_{h_{rd}}, \qquad \text{for all } k, \tag{1}$$

respectively. We highlight that, while all channels for $S \rightarrow R_k$ and $R_k \rightarrow D$ are i.i.d. respectively, we do not assume symmetric channel configuratiaon that $\sigma^2_{h_{sr}} = \sigma^2_{h_{rd}}$. Without losing generality, we assume that the noise variances at all receiving nodes (R_k and D) are the same. As in most existing relay selection approaches, we assume that the destination node has channel state information (CSI) for all channels so that it can choose the best relay node for transmission[2].

In the max-link relay selection, the best transmission link is chosen with the highest channel SNR among all *available* source-to-relay and relay-to-destination links. A source-to-relay link is considered available when the buffer of the corresponding relay node is not full, and a relay-to-destination link is available when the corresponding relay buffer is not empty. If a source-to-relay link is selected, the source

[1]Including the direct link has little effect on the relay selection which is the main issue in this paper.
[2]While the CSI is normally estimated with pilot symbols or channels, this detail is beyond the scope of this paper.

node transmits one data packet to the corresponding relay node, and the relay receives and stores the data packet in its buffer[3]. The number of data packets in the buffer is then increased by one. On the other hand, if a relay-to-destination link is selected, the corresponding relay transmits the earliest stored packet in the buffer to the destination, and the number of packets in the buffer is decreased by one. In general, the best selected relay node R_i (for either reception or transmission) can be expressed as

$$R_{best} = \arg\max_{R_k} \left\{ \bigcup_{R_k:\Psi(Q_k)\neq L} \{|h_{SR_k}|^2\}, \quad \bigcup_{R_k:\Psi(Q_k)\neq 0} \{|h_{R_kD}|^2\} \right\}, \tag{2}$$

where $\Psi(Q_k)$ gives the number of data packets in the buffer Q_k.

Without losing generality, at time slot t, we assume $S \to R_k$ is the strongest link so that the source transmits data packet $s(t)$ to the relay R_k. The received signal at R_k is given by

$$y_{SR_k}(t) = \sqrt{E_s} h_{SR_k}(t) s(t) + n_{R_k}(t), \tag{3}$$

where E_s is the average transmission power at the source and $n_{R_k}(t)$ is the additive-white-Gaussian-noise (AWGN) at R_k with mean zero and variance σ^2.

Then $y_{SR_k}(t)$ is stored into the buffer Q_k and waits for its turn to be transmitted. We assume that at the next τ-th time slot, $y_{SR_k}(t)$ is forwarded from R_k to the destination node. It is clear that $\Psi(Q_k(t)) \leq \tau < \infty$, where $\Psi(Q_k(t))$ gives the number of data packets in the buffer Q_k at time t. Since the relays exploit AF, at the time slot $(t+\tau)$, the received signal at destination is given by

$$y_{R_kD}(t+\tau) = \sqrt{P_{R_k}(t+\tau)} h_{R_kD}(t+\tau) y_{SR_k}(t) + n_D(t+\tau), \tag{4}$$

where $n_D(t+\tau)$ is the noise at the destination node with mean zero and variance σ^2, and $P_{R_k}(t+\tau)$ is the relay gain at R_k which is given by

$$P_{R_k}(t+\tau) = \frac{E_s}{E_s |h_{SR_k}(t)|^2 + \sigma^2}, \tag{5}$$

where we assume all relay nodes have the same average transmission powers as the source node, namely E_s.

[3]The received signal needs to be quantized before it is stored in the buffer. As was mentioned in the introduction, the quantization existing in any half-duplex relays, either AF or DF, with or without buffers. The quantization noise can either be ignored or absorbed in the channel noise.

Substituting (3) into (4) gives

$$y_{R_kD}(t+\tau) = \sqrt{E_s}\sqrt{P_{R_k}(t+\tau)}h_{R_kD}(t+\tau)h_{SR_k}(t)s(t) + n_D(t+\tau) + n'_{R_k}(t), \tag{6}$$

where $n'_{R_k}(t) = \sqrt{P_{R_k}(t+\tau)}h_{R_kD}(t+\tau)n_{R_k}(t)$.

We next derive the outage performance of the buffer aided AF relay system.

III. Outage performance

The outage probability for the AF relay system can be defined as the probability that the instantaneous end-to-end SNR at the destination, γ_D, falls below a certain target SNR γ_{th} such that

$$P_{out} = P(\gamma_D \leq \gamma_{th}), \tag{7}$$

where $P(\cdot)$ denotes the probability of an event. The Markov chain is used to model the transitions between the states of the buffers, where the states describe the number of data packets at every buffer [4]. There are $(L+1)^N$ states in total, and the l^{th} state is expressed as

$$s_l = (\Psi(Q_1)\ \Psi(Q_2)\cdots\Psi(Q_N)), \quad l = 1, \cdots, (L+1)^N. \tag{8}$$

Suppose at time t, the state is at s_j. At time $t+1$, if a source-to-relay link is selected, a packet is transmitted to the selected relay and the number of packets in the corresponding data buffer is increased by 1. On the other hand, if a relay-to-destination link is selected, a packet in the selected relay is forwarded to the destination. Then at the destination, we assume that if the packet can be successfully decoded, it is stored at the destination, or otherwise is discarded[4]. In either case, the number of packets in the selected relay's buffer is decreased by 1. Thus depending on which relay receives or transmits data, at time $t+1$, the buffers may move from state s_j to several possible states. We denote $\mathbb{A}$ as the $(L+1)^N \times (L+1)^N$ state transition matrix, where the entry $\mathbb{A}_{i,j} = P(X_{t+1} = s_i | X_t = s_j)$ which is the transition probability to move from state s_j at time t to state s_i at time $(t+1)$.

We assume that, when the data packet $s(t)$ is transmitted from the source to the destination through the best selected relay R_k, the strongest source-to-relay and relay-to-destination links are selected when the buffer state is at s_i and s_j respectively. It is then from (6) that, the instantaneous end-to-end SNR at

[4]The discarded packet may need to be retransmitted. For example, in the TCP/IP protocol, the re-transmission is handled in the transport layer. The detailed implementation issue is beyond the scope of this paper.

the destination for receiving $s(t)$ is obtained as

$$\gamma_D^{(s_i,s_j)}(t+\tau) = \frac{\gamma_{SR_k}^{(s_i)}(t)\gamma_{R_kD}^{(s_j)}(t+\tau)}{\gamma_{SR_k}^{(s_i)}(t)+\gamma_{R_kD}^{(s_j)}(t+\tau)+1}. \tag{9}$$

where $\gamma_{SR_k}^{(s_i)}(t)$ and $\gamma_{R_kD}^{(s_j)}(t+\tau)$ which are the instantaneous SNRs for $S \to R_k$ and $R_k \to D$ links at time t and $t+\tau$ respectively, and the superscripts $^{(s_i)}$ and $^{(s_j)}$ denote that the corresponding best links are selected when the buffer state is at s_i and s_j respectively. Because we assume all channels at all times are independent fading, for clearer exposition, the time indices t and τ are ignored unless otherwise necessary in the rest of the paper.

By considering all possible states for s_i and s_j, the outage probability of the max-link AF relay selection is given by

$$P_{out} = \sum_{s_i}\sum_{s_j} P(s_i)P(s_j)P(\gamma_D^{(s_i,s_j)} < \gamma_{th}), \tag{10}$$

where $P(s_i)$ and $P(s_j)$ are the probabilities that the buffer state is at s_i and s_j respectively.

Below we show the derivation of $P(\gamma_D^{(s_i,s_j)} < \gamma_{th})$ and $P(s_i)$.

A. $P(\gamma_D^{(s_i,s_j)} < \gamma_{th})$

We suppose at one time the strongest link is selected when the buffer state is at s. The buffer state s uniquely corresponds to a pair of $\{K_{sr}^{(s)}, K_{rd}^{(s)}\}$, where $K_{sr}^{(s)}$ and $K_{rd}^{(s)}$ are the numbers of the available source-to-relay and relay-to-destination links respectively. Recall that a source-to-relay or relay-to-destination link is considered as "unavailable" if the buffer of the corresponding relay node is full or empty respectively.

Because all channels are assumed to independently Rayleigh fading, the instantaneous SNR for every channel, γ_w ($w \in \{SR_k, R_kD\}$), is independently exponentially distributed. Then based on the theory of order statistics [14], the cumulative distribution function (CDF) of the selected channel gain, $\gamma_w^{(s)}$, is given by

$$F_{\gamma_w^{(s)}}(x) = (1-e^{-\frac{x}{\bar{\gamma}_{sr}}})^{K_{sr}^{(s)}} \cdot (1-e^{-\frac{x}{\bar{\gamma}_{rd}}})^{K_{rd}^{(s)}}, \qquad w \in \{SR_k, R_kD\}, \tag{11}$$

where $\bar{\gamma}_{sr} = \frac{E_s\sigma_{h_{sr}}^2}{\sigma^2}$ and $\bar{\gamma}_{rd} = \frac{E_s\sigma_{h_{rd}}^2}{\sigma^2}$ which are the average SNR-s for the source-to-relay and relay-to-destination channels respectively. Differentiating (11) with respect to x gives the probability density function (PDF) of $\gamma_w^{(s)}$ as

$$f_{\gamma_w^{(s)}}(x) = \frac{K_{sr}}{\bar{\gamma}_{sr}} e^{-\frac{x}{\bar{\gamma}_{sr}}} (1 - e^{-\frac{x}{\bar{\gamma}_{sr}}})^{K_{sr}-1} (1 - e^{-\frac{x}{\bar{\gamma}_{rd}}})^{K_{rd}} + \frac{K_{rd}}{\bar{\gamma}_{rd}} e^{-\frac{x}{\bar{\gamma}_{rd}}} (1 - e^{-\frac{x}{\bar{\gamma}_{rd}}})^{K_{rd}-1} (1 - e^{-\frac{x}{\bar{\gamma}_{sr}}})^{K_{sr}}, \qquad w \in \{SR_k, R_k D\}. \tag{12}$$

Supposing the strongest source-to-relay and relay-to-destination links are selected when the buffer state is at s_i and s_j respectively, because all channels are assumed to be mutually independent, we have

$$f_{\gamma_{SR_k}^{(s_i)} \gamma_{R_k D}^{(s_j)}}(x, y) = f_{\gamma_{SR_k}^{(s_i)}}(x) f_{\gamma_{R_k D}^{(s_j)}}(y), \tag{13}$$

Therefore we have

$$P(\gamma_D^{(s_i,s_j)} \leq \gamma_{th}) = \iint\limits_{\frac{xy}{x+y+1} < \gamma_{th}} f_{\gamma_{SR_k}^{(s_i)} \gamma_{R_k D}^{(s_j)}}(x, y)\, dx\, dy, \tag{14}$$

which becomes

$$\begin{aligned} P(\gamma_D^{(s_i,s_j)} < \gamma_{th}) = 1 + &\sum_{\substack{m \\ (m,n) \neq (0,0)}}^{K_{sr}^{(s_i)}} \sum_{n}^{K_{rd}^{(s_i)}} C_{K_{sr}^{(s_i)}}^{m} C_{K_{rd}^{(s_i)}}^{n} (-1)^{m+n} 2 e^{-M_4 \gamma_{th}} \sqrt{M_4 M_{\gamma_{th}}} \cdot \\ &\cdot [\frac{K_{sr}^{(s_j)}}{\bar{\gamma}_{sr}} \sum_{a_1=0}^{K_{sr}^{(s_j)}-1} \sum_{a_2=0}^{K_{rd}^{(s_j)}} (-1)^{a_1+a_2} C_{K_{sr}^{(s_j)}-1}^{a_1} C_{K_{rd}^{(s_j)}}^{a_2} \frac{e^{-M_1 \gamma_{th}}}{\sqrt{M_1}} \mathcal{B}(1, 2\sqrt{M_1 M_4 M_{\gamma_{th}}}) \\ &+ \frac{K_{rd}^{(s_j)}}{\bar{\gamma}_{rd}} \sum_{a_3=0}^{K_{rd}^{(s_j)}-1} \sum_{a_4=0}^{K_{sr}^{(s_j)}} (-1)^{a_3+a_4} C_{K_{rd}^{(s_j)}-1}^{a_3} C_{K_{sr}^{(s_j)}}^{a_4} \frac{e^{-M_2 \gamma_{th}}}{\sqrt{M_2}} \mathcal{B}(1, 2\sqrt{M_2 M_4 M_{\gamma_{th}}})], \end{aligned} \tag{15}$$

where

$$M_1 = \frac{1}{\bar{\gamma}_{sr}} + \frac{a_1}{\bar{\gamma}_{sr}} + \frac{a_2}{\bar{\gamma}_{rd}}, M_2 = \frac{1}{\bar{\gamma}_{rd}} + \frac{a_3}{\bar{\gamma}_{rd}} + \frac{a_4}{\bar{\gamma}_{sr}}, M_4 = \frac{m}{\bar{\gamma}_{sr}} + \frac{n}{\bar{\gamma}_{rd}}, M_{\gamma_{th}} = \gamma_{th}(\gamma_{th} + 1), \tag{16}$$

and $\mathcal{B}$ denotes the modified Bessel function of the second kind [15].

Proof see Appendix.

B. $P(s_i)$

Because the average channel gains for the $S \to R_k$ and $R_k \to D$ links are not the same, at any time the probabilities to select the source-to-relay and relay-to-destination transmission are also not the same. This is very different from existing buffer-aided relay selection schemes (e.g. the max-link approach in [4]) where the selection of any available link is equally likely. With this observation, we divide all states which can be moved from s_l into two sets, U_l^+ and U_l^-, where U_l^+ contains all states to which s_l can move when a source-to-relay link is selected and U_l^- contains all states to which s_l can move when a relay-to-destination link is selected. We let $p_{S\to R}^{(s_l)}$ and $p_{R\to D}^{(s_l)}$ be the probabilities that the source-to-relay and relay-to-destination transmissions are selected at state s_l, respectively. It is clear that $p_{S\to R}^{(s_l)} + p_{R\to D}^{(s_l)} = 1$.

On the other hand, because we assume all source-to-relay channels are i.i.d. fading and all relay-to-destination channels are also i.i.d. fading, the selection of one particular link within either U_l^+ or U_l^- is equally likely. Therefore, the probability to select a source-to-relay or relay-to-destination link at state s_l is given by

$$\begin{aligned} p_+^{(s_l)} &= \left(\frac{1}{K_{sr}^{(s_l)}} p_{S\to R}^{(s_l)}\right) = \frac{1}{K_{sr}^{(s_l)}}(1 - p_{R\to D}^{(s_l)}), \\ p_-^{(s_l)} &= \left(\frac{1}{K_{rd}^{(s_l)}} p_{R\to D}^{(s_l)}\right) = \frac{1}{K_{rd}^{(s_l)}} p_{R\to D}^{(s_l)}, \end{aligned} \tag{17}$$

respectively.

With these observations, the (i,j)-th entry of the state transition matrix $\mathbb{A}$ is expressed as

$$\mathbb{A}_{i,j} = \begin{cases} p_+^{(s_j)} = \frac{1}{K_{sr}^{(s_j)}}(1 - p_{R\to D}^{(s_j)}), & \text{if} \quad s_i \in U_j^+, \\ p_-^{(s_j)} = \frac{1}{K_{rd}^{(s_j)}} p_{R\to D}^{(s_j)}, & \text{if} \quad s_i \in U_j^-. \\ 0, & \text{elsewhere}, \end{cases} \tag{18}$$

Because the transition matrix $\mathbf{A}$ in (18) is column stochastic and irreducible[5], the stationary state probability vector is obtained as (see [17], [18])

$$\boldsymbol{\pi} = (\mathbf{A} - \mathbf{I} + \mathbf{B})^{-1}\mathbf{b}, \tag{19}$$

where $\boldsymbol{\pi} = [\pi_1, \cdots, \pi_{(L+1)^K}]^{\mathrm{T}}$, $\mathbf{b} = (1, 1, ..., 1)^T$, $\mathbf{I}$ is the identity matrix and $\mathbf{B}_{n,l}$ is an $n \times l$ all one matrix. Or in the stationary state, we have $\pi_l = \lim_{t\to\infty} P(s_l)$ for $l = 1, \cdots, (L+1)^K$.

Below we derive $p_{R\to D}^{(s_l)}$ in (18).

C. $p_{R\to D}^{(s_l)}$: probability of selecting the relay-to-destination transmission at state s_l

If there are no relay-to-destination links available (or $K_{rd}^{(s_l)} = 0$), we have $p_{R\to D}^{(s_l)} = 0$. On the other hand, if there are no source-to-relay links available (or $K_{sr}^{(s_l)} = 0$), we have $p_{R\to D}^{(s_l)} = 1$. For other cases,

[5] *Column stochastic* means all entries in any column sum up to one, *irreducible* means that it is possible to move from any state to any state [16], [17].

$p_{R\to D}^{(s_l)}$ is given by

$$
\begin{aligned}
p_{R\to D}^{(s_l)} = P(x<y) &= \iint\limits_{x<y} f_{XY}(x,y)dxdy \\
&= \int_0^{\infty}\int_0^{y} f_{XY}(x,y)dxdy,
\end{aligned}
\tag{20}
$$

where x and y are the maximum SNR-s from the $K_{sr}^{(s_l)}$ number of source-to-relay and $K_{rd}^{(s_l)}$ number of relay-to-destination links respectively, and $f_{XY}(x,y)$ is the joint PDF of x and y. Because x and y are mutually independent, we have

$$
f_{XY}(x,y) = f_X(x)f_Y(y) = \frac{K_{sr}^{(s_l)}K_{rd}^{(s_l)}}{\bar{\gamma}_{sr}\bar{\gamma}_{rd}} e^{-(\frac{x}{\bar{\gamma}_{sr}}+\frac{y}{\bar{\gamma}_{rd}})}(1-e^{-\frac{x}{\bar{\gamma}_{sr}}})^{K_{sr}^{(s_l)}-1}(1-e^{-\frac{y}{\bar{\gamma}_{rd}}})^{K_{rd}^{(s_l)}-1}. \tag{21}
$$

where $f_X(x)$ and $f_Y(y)$ are the PDF-s of x and y respectively. Substituting (21) into (20) gives

$$
\begin{aligned}
&p_{R\to D}^{(s_l)} = \int_0^{\infty}\int_0^{y} \frac{K_{sr}^{(s_l)}K_{rd}^{(s_l)}}{\bar{\gamma}_{sr}\bar{\gamma}_{rd}} e^{-(\frac{x}{\bar{\gamma}_{sr}}+\frac{y}{\bar{\gamma}_{rd}})}(1-e^{-\frac{x}{\bar{\gamma}_{sr}}})^{K_{sr}^{(s_l)}-1}(1-e^{-\frac{y}{\bar{\gamma}_{rd}}})^{K_{rd}^{(s_l)}-1}dxdy \\
&= \frac{K_{rd}^{(s_l)}}{\bar{\gamma}_{rd}}\int_0^{\infty} e^{-\frac{y}{\bar{\gamma}_{rd}}}(1-e^{-\frac{y}{\bar{\gamma}_{rd}}})^{K_{rd}^{(s_l)}-1}(1-e^{-\frac{y}{\bar{\gamma}_{sr}}})^{K_{sr}^{(s_l)}}dy.
\end{aligned}
\tag{22}
$$

Applying a binomial expansion on $(1-e^{-\frac{y}{\bar{\gamma}_{rd}}})^{K_{rd}^{(s_l)}-1}$ and $(1-e^{-\frac{y}{\bar{\gamma}_{sr}}})^{K_{sr}^{(s_l)}}$ gives

$$
\begin{aligned}
(1-e^{-\frac{y}{\bar{\gamma}_{rd}}})^{K_{rd}^{(s_l)}-1} &= \sum_{m=0}^{K_{rd}^{(s_l)}-1} C^m_{K_{rd}^{(s_l)}-1}(-1)^m e^{-\frac{ym}{\bar{\gamma}_{rd}}}, \\
(1-e^{-\frac{y}{\bar{\gamma}_{sr}}})^{K_{sr}^{(s_l)}} &= \sum_{n=0}^{K_{sr}^{(s_l)}} C^n_{K_{sr}^{(s_l)}}(-1)^n e^{-\frac{yn}{\bar{\gamma}_{sr}}}.
\end{aligned}
\tag{23}
$$

Then we obtain

$$
\begin{aligned}
p_{R\to D}^{(s_l)} &= \frac{K_{rd}^{(s_l)}}{\bar{\gamma}_{rd}}\sum_{m=0}^{K_{rd}^{(s_l)}-1}\sum_{n=0}^{K_{sr}^{(s_l)}} C^m_{K_{rd}^{(s_l)}-1}C^n_{K_{sr}^{(s_l)}}(-1)^{m+n}\int_0^{\infty} e^{-\frac{y}{\bar{\gamma}_{rd}}-\frac{ym}{\bar{\gamma}_{rd}}-\frac{yn}{\bar{\gamma}_{sr}}}dy \\
&= \sum_{m=0}^{K_{rd}^{(s_l)}-1}\sum_{n=0}^{K_{sr}^{(s_l)}} C^m_{K_{rd}^{(s_l)}-1}C^n_{K_{sr}^{(s_l)}}(-1)^{m+n}\frac{K_{rd}^{(s_l)}\cdot\bar{\gamma}_{sr}}{\bar{\gamma}_{sr}+\bar{\gamma}_{sr}\cdot m+\bar{\gamma}_{rd}\cdot n}
\end{aligned}
\tag{24}
$$

D. A special case: symmetric $S\to R$ and $R\to D$ channels with $\sigma^2_{h_{sr}}=\sigma^2_{h_{rd}}$

In this section, we consider a special case that the average channel gains for the source-to-relay and relay-to-destination links are the same, or $\sigma^2_{h_{sr}}=\sigma^2_{h_{rd}}$. Under this symmetric channel scenario, the probabilities to select any available source-to-relay and relay-to-destination link at state s_l at any time are the same. Thus (17) can be simplified as

$$
p^+_{s_l} = p^-_{s_l} = \frac{1}{K^{(s_l)}}, \qquad l=1,\cdots,(L+1)^N, \tag{25}
$$

where $K^{(s_l)} = K_{sr}^{(s_l)} + K_{rd}^{(s_l)}$ which is the total number of the available links (including both source-to-relay and relay-to-destination links) at state s_l. Then the state transition matrix is given by

$$\mathbb{A}_{i,j} = \begin{cases} \frac{1}{K^{(s_j)}}, & \text{if} \quad s_i \in U_j, \\ 0, & \text{elsewhere}, \end{cases} \qquad j = 1, \cdots, (L+1)^N, \tag{26}$$

where U_j is the set of all possible states to which can be moved from s_j at the next time slot.

The stationary state probability vector is then obtained by substituting (26) into (19). Alternatively, because at any time the probability to select one available link is uniform and every link corresponds to one transition of states, the stationary probability for a state is proportional to its corresponding number of available links so that we have

$$\pi_j = \lim_{t\to\infty} P(s_j) = \frac{K^{(s_j)}}{\sum_{l=1}^{(L+1)^N} K^{(s_l)}}. \tag{27}$$

For the proof of (27) please refer to Chapter 11 Section 3 Ergodic Markov Chains in [16].

Next, we need to calculate the outage probability for the "symmetric" channel, $P_{symmetric}(\gamma_D^{(s_i,s_j)} < \gamma_{th})$, when the strongest source-to-relay and relay-to-destination links are selected at state s_i and s_j respectively. By letting $\bar{\gamma} = \bar{\gamma}_{sr} = \bar{\gamma}_{rd}$, and following the similar procedure in Section III-A, we can obtain

$$\begin{aligned} P_{symmetric}(\gamma_D^{(s_i,s_j)} < \gamma_{th}) =& 1 + \frac{K^{(s_j)}}{\bar{\gamma}} \cdot \sum_{n=0}^{K^{(s_j)}-1} \sum_{m=1}^{K^{(s_i)}} C_{K^{(s_j)}-1}^{n} C_{K^{(s_i)}}^{m} (-1)^{m+n} 2e^{-\frac{\gamma_{th}}{\bar{\gamma}}(1+m+n)} \cdot \\ & \cdot \sqrt{\frac{m\gamma_{th}(\gamma_{th}+1)}{(n+1)}} \mathcal{B}\left(1, \frac{2}{\bar{\gamma}}\sqrt{m\gamma_{th}(\gamma_{th}+1)(n+1)}\right). \end{aligned} \tag{28}$$

Finally, substituting (27) and (28) into (10) gives the overall outage probability for the symmetric channel configuration as

$$\begin{aligned} P_{out}^{\text{symmetric}} =& \sum_{s_i}\sum_{s_j} \frac{K^{(s_i)}}{\sum_{l=1}^{(L+1)^N} K^{(s_l)}} \cdot \frac{K^{(s_j)}}{\sum_{l=1}^{(L+1)^N} K^{(s_l)}} \left(1 + \frac{K^{(s_j)}}{\bar{\gamma}} \sum_{n=0}^{K^{(s_j)}-1} \sum_{m=1}^{K^{(s_i)}} C_{K^{(s_j)}-1}^{n} C_{K^{(s_i)}}^{m} \cdot \right. \\ & \left. \cdot (-1)^{m+n} 2e^{-\frac{\gamma_{th}}{\bar{\gamma}}(1+m+n)} \sqrt{\frac{m\gamma_{th}(\gamma_{th}+1)}{(n+1)}} \mathcal{B}\left(1, \frac{2}{\bar{\gamma}}\sqrt{m\gamma_{th}(\gamma_{th}+1)(n+1)}\right)\right). \end{aligned} \tag{29}$$

IV. Average Packet Delay

In the AF max-link scheme, at a transmission node (either the source or a relay), a data packet can only be transmitted out if the corresponding link is selected. This brings up 2 issues: first, the packets may not arrive at the destination in order; second, each packet may suffer from different delay within the systems. While the first issue can be easily handled by for instance numbering every packet, the delay becomes a main issue in buffer-aided relay selection systems [8].

In general, a packet delay includes delays at both the source and selected relay nodes, which are denoted as D_s and D_r respectively. A simple example is illustrated in Fig. 2, where there are 3 packets ($s(1), s(2)$ and $s(3)$) transmitted out consecutively from the source. The transmission time-span for every packets is represented by a horizontal bar in Fig. 2, where D_s and D_r indicate the delay time slots at the source and relay nodes respectively, $S-R$ and $R-D$ indicate the transmission time slots for source-to-relay and relay-to-destination respectively. For example, packet s_1 is transmitted from the source to a relay node at time slot 2. After that, packet s_2 waits for 3 time slots (slots 3, 4 and 5) and is then transmitted to a relay. After s_2 arrives the relay at slot 6, it waits for another 4 time slots (slots 7-10) before it is eventually transmitted to the destination at slot 11. Thus the delays for s_2 at the source and relay nodes are 3 and 4 respectively in this example. Fig. 2 also shows that the packets arrive at the destination in the order of $[s_1, s_3, s_2]$, which is clearly not as same as the transmission order.

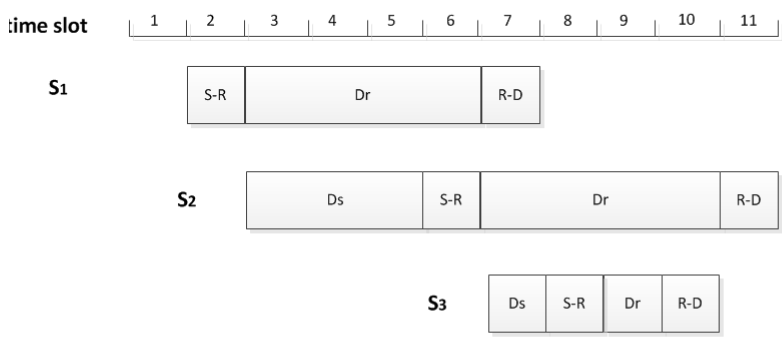

Fig. 2. An example of packet delay in the AF max-link scheme.

We particularly highlight that, while different packet may suffer from different delay, the system throughput (or the average data rate) of the AF max-link scheme is not scarified. This is because that, at any time slot, there is always one link selected for transmission. Therefore, when a packet is "waiting" for transmission at a node, another packet must be transmitted at another node. Suppose there are M packets in total. Because each packet takes 2 time slots for transmission (excluding the waiting time), if M is large enough, the overall transmission time to deliver all packets is approximately $2M$. Therefore, the system average throughput is $\eta = \frac{M}{2M} = 0.5$, which is the same as that for the classic 3-node "$S \to R \to D$" relay system [19].

According to the Little's law [**?**], the average packet delay at the node i can be obtained as

$$\mathrm{E}[D_i] = \frac{\mathrm{E}[Q_i]}{\eta_i}, \tag{30}$$

where $\mathrm{E}[Q_i]$ and η_i are the average queuing length and throughput at the node.

In the following two subsections, we derive the average packet delay at the source and relay nodes respectively.

A. Average packet delay at the source

Because all data are transmitted from the same source node, the average throughput at the source node is the same as that for the overall system which is given by

$$\eta_s = \eta = 1/2 \tag{31}$$

On the other hand, if we assume that the source always has data to transmit, the queuing length at the source depends on how fast the data leave the source, which again depends on the probability that a source-to-relay link is selected. Considering all buffer states at the relay, the probability that a source-to-relay link is selected can be obtained as $p_{S\to R} = \sum_{l=1}^{(L+1)^N} \pi_l \cdot p_{S\to R}^{(s_l)} = \sum_{s_l} P(s_l) \cdot (1 - p_{R\to D}^{(s_l)})$, where π_l is the stationary probability for state s_l which is obtained in (19), and $p_{R\to D}^{(s_l)}$ is the probability to select a relay-to-destination link at state s_l which is given by (24). Alternatively, for any fixed sized buffers, the number of data arriving at the whole the relays must be equal to that leaving these relays, because no data can stay in a relay node forever and fails to reach the source. Thus we must have

$$p_{S\to R} = p_{R\to D} = 1/2 \tag{32}$$

This implies that the average queuing length at the source node is

$$\mathrm{E}[Q_s] = 1/2 \tag{33}$$

Substituting (31) and (33) into (30) gives the average packet delay at the source node as

$$\mathrm{E}[D_s] = \frac{\mathrm{E}[Q_s]}{\eta_s} = 1. \tag{34}$$

We highlight that (34) holds for both symmetric and asymmetric channel scenarios.

B. Average packet delay at the relay

Because the probabilities to select any of the relays are the same, the average packet delays at any of the relay are also the same, so is the average throughput at any relay which is given by

$$\eta_r = \frac{\eta}{N} = \frac{1}{2N} \tag{35}$$

Let $Q_r^{(s_l)}$ be the queuing length (or the average number of packets) for the selected relay at the buffer state s_l. Considering all buffer state s_l, the average queuing length at the selected relay is obtained as

$$\mathrm{E}[Q_r] = \sum_{l=1}^{(L+1)^N} \pi_l Q_r^{(s_l)}, \tag{36}$$

Substituting (35) and (36) into (30) gives the average packet delay at the relay as

$$\mathrm{E}[D_r] = \frac{1}{2N} \sum_{l=1}^{(L+1)^N} \pi_l Q_r^{(s_l)} \tag{37}$$

Finally combining the delay at the source and relay nodes gives the overall average delay in the AF max-link system as

$$\mathrm{E}[D] = \mathrm{E}[D_s] + \mathrm{E}[D_r] = 1 + \frac{1}{2N} \sum_{l=1}^{(L+1)^N} \pi_l Q_r^{(s_l)}. \tag{38}$$

On the other hand, if the source-to-relay and relay-to-destination channels are symmetric (i.e. $\sigma_{h_{sr}}^2 = \sigma_{h_{rd}}^2$), the average packet delay at the relay in (37) can be obtained as $\mathrm{E}[D_r] = L/2$, and the the overall average delay becomes $\mathrm{E}[D] = 1 + NL$.

C. Numerical example

We have done extensive numerical simulation which all well match the above delay analysis. Some of the results are shown in Table I and II, where for fair comparison, we let $\bar{\gamma}_{sr}(\mathrm{dB}) + \bar{\gamma}_{rd}(\mathrm{dB}) = 40$dB in all cases. It is clearly shown that, with more relay number N and larger buffer size L, we have larger delays. Moreover, if the relay-to-destination link SNR is stronger than the source-to-relay SNB, we have smaller delay. This is not surprising because higher relay-to-destination SNR implies that the relay-to-destination link is more likely to be selected and the data is more quickly forwarded to the destination.

TABLE I

AVERAGE PACKET DELAYS

$(N, L) = (2, 2)$	D_{ave}	
$(\bar{\gamma}_{sr}, \bar{\gamma}_{rd})$	Simulation	Theory
10 30	2.0313	2.0300
15 25	2.2984	2.2999
20 20	4.9939	5
25 15	7.6987	7.7001
30 10	7.9706	7.9700

TABLE II

AVERAGE PACKET DELAYS

$(N, L) = (4, 4)$	D_{ave}	
$(\bar{\gamma}_{sr}, \bar{\gamma}_{rd})$	Simulation	Theory
10 30	2.0401	2.0416
15 25	2.4263	2.4273
20 20	17.0481	17
25 15	31.5646	31.5727
30 10	31.9534	31.9584

V. DIVERSITY ORDER

In order to show the diversity order of the AF max-link scheme, we assume all channels are i.i.d such that $\sigma^2_{h_{sr}} = \sigma^2_{h_{rd}} = \sigma^2_h$, and then the outage probability is given in (29). The diversity order can be defined as

$$r = -\lim_{\bar{\gamma}_h \to \infty} \frac{\log P_{out}}{\log \bar{\gamma}_h}, \tag{39}$$

where $\bar{\gamma}_h = (E_s \sigma^2_h)/\sigma^2$ which is the average SNR for every channel. However substituting (29) into (39) does not explicitly shows the diversity order. Instead, we first derive the upper and lower bounds of the outage probability, from which the diversity order is obtained; then we show that the minimum and maximum diversity orders are obtained when the relay buffer sizes are 1 and ∞ respectively.

A. Outage probability bounds

Noting $\gamma^{(s_i)}_{SR_k} = \bar{\gamma}_h |h_{SR_k}|^2$, $\gamma^{(s_j)}_{R_kS} = \bar{\gamma}_h |h_{R_kD}|^2$, and from (9), we have

$$\lim_{\bar{\gamma}_h \to \infty} \gamma^{(s_i,s_j)}_D = \frac{\gamma^{(s_i)}_{SR_k} \gamma^{(s_j)}_{R_kD}}{\gamma^{(s_i)}_{SR_k} + \gamma^{(s_j)}_{R_kD}}. \tag{40}$$

Since $\gamma_{SR_k}^{(s_i)} > 0$ and $\gamma_{R_kD}^{(s_j)} > 0$, we have

$$\frac{1}{2}\min(\gamma_{SR_k}^{(s_i)}, \gamma_{R_kD}^{(s_j)}) \leq \frac{\gamma_{SR_k}^{(s_i)}\gamma_{R_kD}^{(s_j)}}{\gamma_{SR_k}^{(s_i)} + \gamma_{R_kD}^{(s_j)}} \leq \min(\gamma_{SR_k}^{(s_i)}, \gamma_{R_kD}^{(s_j)}). \tag{41}$$

From (40) and (41), we have

$$P_e^L \leq \lim_{\bar{\gamma}_h \to \infty} P(\gamma_D^{(s_i,s_j)} < \gamma_{th}) \leq P_e^U, \tag{42}$$

where $P_e^L = P(\min(\gamma_{SR_k}^{(s_i)}, \gamma_{R_kD}^{(s_j)}) < \gamma_{th})$ and $P_e^U = P(1/2 \cdot \min(\gamma_{SR_k}^{(s_i)}, \gamma_{R_kD}^{(s_j)})$ which are the lower and upper bounds for $\lim_{\bar{\gamma}_h \to \infty} P(\gamma_D^{(s_i,s_j)} < \gamma_{th})$ respectively.

Supposing the total numbers of available links for buffer state s_i and s_j are given by $K^{(s_i)}$ and $K^{(s_j)}$ respectively, the lower bound P_e^L can be obtained as

$$\begin{aligned} P_e^L &= P(\min(\gamma_{SR_k}^{(s_i)}, \gamma_{R_kD}^{(s_j)}) < \gamma_{th}) \\ &= 1 - (1 - F_X(\gamma_{th}))(1 - F_Y(\gamma_{th})) \\ &= (1 - e^{-\frac{\gamma_{th}}{\bar{\gamma}_h}})^{K^{(s_i)}} + (1 - e^{-\frac{\gamma_{th}}{\bar{\gamma}_h}})^{K^{(s_j)}} - (1 - e^{-\frac{\gamma_{th}}{\bar{\gamma}_h}})^{K^{(s_i)}}(1 - e^{-\frac{\gamma_{th}}{\bar{\gamma}_h}})^{K^{(s_j)}}. \end{aligned} \tag{43}$$

Further noting that $e^x \approx 1 + x$ for very small x, and ignoring the high order terms, we have

$$\lim_{\bar{\gamma}_h \to \infty} P_e^L = \left(\frac{\gamma_{th}}{\bar{\gamma}_h}\right)^{\min\{K^{(s_i)}, K^{(s_j)}\}}. \tag{44}$$

Then we have $-\lim_{\bar{\gamma}_h \to \infty} \frac{\log P_e^L}{\log \bar{\gamma}_h} = \min\{K^{(s_i)}, K^{(s_j)}\}$. Further noting that $N \leq K^{(s_i)} \leq 2N$ and $N \leq K^{(s_j)} \leq 2N$, we have

$$N \leq -\lim_{\bar{\gamma}_h \to \infty} \frac{\log P_e^L}{\log \bar{\gamma}_h} \leq 2N. \tag{45}$$

On the other hand, the upper bound P_e^U can be obtained as

$$\begin{aligned} P_e^U &= P(1/2 \cdot \min(\gamma_{SR_k}^{(s_i)}, \gamma_{R_kD}^{(s_j)}) < \gamma_{th}) \\ &= 1 - (1 - F_X(2\gamma_{th}))(1 - F_Y(2\gamma_{th})) \\ &= (1 - e^{-\frac{2\gamma_{th}}{\bar{\gamma}_h}})^{K^{(s_i)}} + (1 - e^{-\frac{2\gamma_{th}}{\bar{\gamma}_h}})^{K^{(s_j)}} - (1 - e^{-\frac{2\gamma_{th}}{\bar{\gamma}_h}})^{K^{(s_i)}}(1 - e^{-\frac{2\gamma_{th}}{\bar{\gamma}_h}})^{K^{(s_j)}}, \end{aligned} \tag{46}$$

Then following the similar procedure as that for P_e^L, we have

$$\lim_{\bar{\gamma}_h \to \infty} P_e^U = \left(\frac{\gamma_{th}}{\bar{\gamma}_h}\right)^{\min\{K^{(s_i)}, K^{(s_j)}\}}, \tag{47}$$

and

$$N \leq -\lim_{\bar{\gamma}_h \to \infty} \frac{\log P_e^U}{\log \bar{\gamma}_h} \leq 2N. \tag{48}$$

It is clear from (44) and (47) that, when $\bar{\gamma}_h \to \infty$, $\log P_e^L$ and $\log P_e^U$ have the same gradients against $\log \bar{\gamma}_h$. Then using (45) and (48) in (42), we must have

$$N \leq -\lim_{\bar{\gamma}_h \to \infty} \frac{\log P(\gamma_D^{(s_i,s_j)} < \gamma_{th})}{\log \bar{\gamma}_h} \leq 2N. \tag{49}$$

Particularly, if $K^{(s_i)} = K^{(s_j)} = K$, we have

$$-\lim_{\bar{\gamma}_h \to \infty} \frac{\log P(\gamma_D^{(K,K)} < \gamma_{th})}{\log \bar{\gamma}_h} = K. \tag{50}$$

Finally, because (49) holds for every s_i and s_j, from (10), the diversity order of the max-link AF relay selection can be obtained as

$$N \leq r \leq 2N. \tag{51}$$

It is clear that the diversity order r is a function of both the relay number N and buffer size L. Below we show the upper and lower limits of the diversity order are reached when $L = 1$ and $L \to \infty$ respectively.

B. Buffer size $L = 1$

If the buffer size $L = 1$, the available number of links at any state is N, or we have $P(K^{(s_i)} = N) = 1$ for all s_i. Then from (10), the outage probability is given by

$$P_{out}^{(L=1)} = P(\gamma_D^{(N,N)} < \gamma_{th}). \tag{52}$$

Furthermore from (50), we have the diversity order for $L = 1$ as

$$r = -\lim_{\bar{\gamma}_h \to \infty} \frac{P_{out}^{(L=1)}}{\log \bar{\gamma}_h} = N. \tag{53}$$

C. Buffer size $L \to \infty$

If the buffer size is L, there are $(L-1)^N$ states which are neither full nor empty so that their corresponding number of available links is $2N$. Since the total number of buffer states is $(L+1)^N$, the number of states whose corresponding links is not $2N$ is $(L+1)^N - (L-1)^N$. Thus the probability that the available link is not $2N$ is given by

$$P(K \neq 2N) = \sum_{K^{(s_j)} \neq 2N} \pi_j, \tag{54}$$

where $K^{(s_j)}$ and π_j are the total number of available links and stationary probability for the state s_j respectively. Substituting (27) into (54), and recalling that $N \leq K^{(s_j)} \leq 2N$ for all j, we have

$$\begin{aligned} P(K \neq 2N) &= \sum_{K^{(s_j)} \neq 2N} \frac{K^{(s_j)}}{\sum_{l=1}^{(L+1)^N} K^{(s_l)}} \\ &\leq \sum_{D_j \neq 2N} \frac{2N}{\sum_{l=1}^{(L+1)^N} N} = 2 \cdot \frac{(L+1)^N - (L-1)^N}{(L+1)^N - 1}. \end{aligned} \tag{55}$$

It is clear from (55) that $\lim_{L\to\infty} P(K \neq 2N) = 0$.

Therefore, if $L \to \infty$, the outage probability in (10) can be simplified as

$$P_{out}^{(L\to\infty)} = P(\gamma_D^{(2N,2N)} < \gamma_{th}). \tag{56}$$

Then from (50), we obtain the diversity order for $L \to \infty$ as

$$r = -\lim_{\bar{\gamma}_h \to \infty} \frac{P_{out}^{(L\to\infty)}}{\log \bar{\gamma}_h} = 2N. \tag{57}$$

VI. Coding gain

Compared with the traditional max-SNR relay selection scheme, the AF max-link scheme has not only diversity but also coding gain. In order to highlight the coding gain, we assume the relay buffer size of the max-link scheme is $L = 1$. Then the diversity orders for both the max-link and max-SNR schemes are N, and the outage performance advantage of the AF max-link over the max-SNR scheme comes from the coding gain.

From (52), when $L = 1$, the outage probability of the AF max-link scheme is given by $P_{out}^{(L=1)} = P(\gamma_D^{(N,N)} < \gamma_{th})$ whose lower and upper bounds (P_e^L and P_e^U respectively) can be obtained using (42). As is shown in Section V-A, when the channel SNR $\bar{\gamma}_h \to \infty$, $\log P_e^L$ and $\log P_e^U$ have the same gradients against $\log \bar{\gamma}_h$. This implies that, for $\bar{\gamma}_h \to \infty$, we must have

$$10 \log P_{out}^{(L=1)} = \alpha + 10 \log P_e^L, \tag{58}$$

where $0 \leq \alpha \leq \log(P_e^U / P_e^L)$ which is a small constant.

We note that, $e^x \approx 1 + x$ for very small x. Substituting (43) into (58), and ignoring the high order terms at the high SNR, we have

$$\lim_{\bar{\gamma}_h \to \infty} 10 \log P_{out}^{(L=1)} = \alpha + 10 \log \left[2 \cdot \left(\frac{\gamma_{th}}{\bar{\gamma}_h} \right)^N \right] \tag{59}$$

On the other hand, in the traditional max-SNR scheme, the best relay is selected that maximizes the SNR at the destination. To be specific, if the relay R_k is selected, the end-to-end SNR at the destination can be obtained as

$$\gamma_D^{(R_k)} = \frac{\gamma_{SR_k} \gamma_{R_k D}}{\gamma_{SR_k} + \gamma_{R_k D} + 1}, \tag{60}$$

where γ_{SR_k} and $\gamma_{R_k D}$ are the instantaneous channel SNR for $S \to R_k$ and $R_k \to D$ links respectively. Similar to (42), we can obtain the lower and upper bounds for $P(\gamma_D^{(R_k)} < \gamma_{th})$ at the high SNR as

$$P(\min(\gamma_{SR_k}, \gamma_{R_k D}) < \gamma_{th}) \leq P(\gamma_D^{(R_k)} < \gamma_{th}) \leq P(1/2 \cdot \min(\gamma_{SR_k}, \gamma_{R_k D}) < \gamma_{th}). \tag{61}$$

Because the best relay in the max-SNR scheme is selected among N pair of source-to-relay and relay-to-destination links that maximizes (60), the outage probability can be obtained as

$$P_{out}^{(max-SNR)} = [P(\gamma_D^{(R_k)} < \gamma_{th})]^N \tag{62}$$

Substituting (61) into (62) gives

$$[P(\min(\gamma_{SR_k}, \gamma_{R_k D}) < \gamma_{th})]^N \leq P_{out}^{(max-SNR)} \leq [P(1/2 \cdot \min(\gamma_{SR_k}, \gamma_{R_k D}) < \gamma_{th})]^N. \tag{63}$$

For the similar reasons in obtaining (58), at the high SNR, we must have

$$10 \log P_{out}^{(max-SNR)} = \beta + 10 \log [P(\min(\gamma_{SR_k}, \gamma_{R_k D}) < \gamma_{th})]^N \tag{64}$$

where β is a small positive constant. Because the channel SNR are exponentially distributed, we have

$$[P(\min(\gamma_{SR_k}, \gamma_{R_k D}) < \gamma_{th})]^N = \left((1 - e^{-\frac{\gamma_{th}}{\bar{\gamma}_h}}) + (1 - e^{-\frac{\gamma_{th}}{\bar{\gamma}_h}}) - (1 - e^{-\frac{\gamma_{th}}{\bar{\gamma}_h}})(1 - e^{-\frac{\gamma_{th}}{\bar{\gamma}_h}}) \right)^N. \tag{65}$$

Substituting (65) into (64), and ignoring the high orders at the high SNR, we have

$$\lim_{\bar{\gamma}_h \to \infty} 10 \log P_{out}^{(max-SNR)} = \beta + 10 \log \left(2 \cdot \frac{\gamma_{th}}{\bar{\gamma}_h} \right)^N \tag{66}$$

Finally from (59) and (66), when the buffer size $L = 1$, the coding gain of the AF max-link scheme over the traditional AF max-SNR scheme is given by

$$\begin{aligned}\theta^{(L=1)}(\text{dB}) &= \lim_{\bar{\gamma}_h \to \infty} \left(10 \log P_{out}^{(max-SNR)} - 10 \log P_{out}^{(L=1)}\right) \\ &= 10(N-1)\log 2 + (\beta - \alpha) \\ &\approx 10(N-1)\log 2,\end{aligned} \tag{67}$$

where the approximation in (67) comes from the fact that both α and β are small positive constants.

We recall that the data buffers (with size 1) also exist at the relays in traditional relay selection scheme, because the data need to be stored in the relay at one time and forwarded to the destination at the next time. It is clear from (67) that, even with $L = 1$, the AF max-link still has better outage performance than the traditional AF max-SNR scheme because of the coding gain. It is also shown in (67) that more relays lead to higher coding gain. Only when $N = 1$, does the coding gain disappear because then both the max-link and max-AF schemes reduce to the standard 3 nodes relay system.

While the coding gain analysis above is for buffer size $L = 1$, it is also useful in understanding more general case with other buffer sizes, where the coding gain also exists. In general, the coding gain depends on the number of available links for selection, which again depends on both the relay number N and buffer sizes L. With larger L and N, we have larger coding gain. This will be verified in the simulation later in this paper.

VII. Simulation and discussions

In this section, numerical results are shown to verify the analysis in this paper. In the simulations below, the average transmission powers for all transmission nodes is set as $E_s = 1$, the noise variances for all receiving nodes are set as $\sigma^2 = 1$. All simulation results are obtained with 1,000,000 independent runs.

A. *Outage performance of the AF max-link scheme*

Fig. 3 verifies the outage probability expression in (29) with simulation results under varies scenarios. It is clearly shown that in all cases the theoretical analysis well matches the simulation results. Both Fig. 3 (a) and (b) show that the best outage performance is obtained when the source-to-relay and relay-to-destination channels are symmetric.

Fig. 4 (a) and (b) show the outage performance against different buffer lengths L for symmetric and asymmetric channel configurations respectively, where the relay number is fixed at $N = 3$. It is clearly

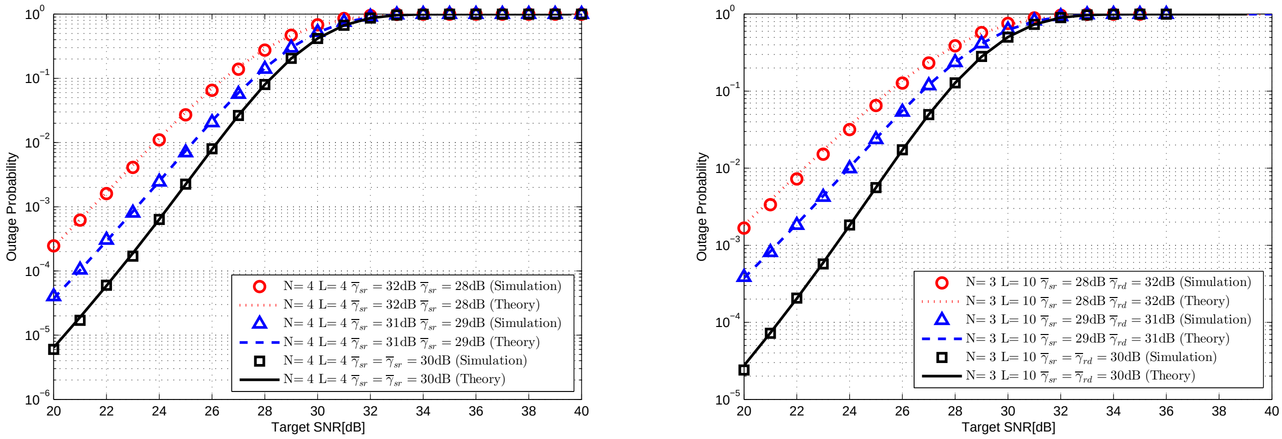

(a) $N = 4,\ L = 4$ (b) $N = 3,\ L = 10$

Fig. 3. Outage probability performance of the AF max-link scheme: theory *vs* simulation.

shown that the outage performance improves with larger buffer size L, but the improvement is less significant when L becomes larger. It is shown in Fig. 4 (a) and (b) that, when $L = 50$ and $L = 20$, the outage performance is almost as same as that for $L \to \infty$ for the asymmetric and symmetric channel configuration respectively. Therefore, in practice, the full outage order $2N$ can be achieved with finite buffer sizes. It is also shown that, with larger buffer size L, the outage performance improvement in the symmetric channel (Fig. 4 (a)) is much more significant than that in the asymmetric channel (Fig. 4 (b)).

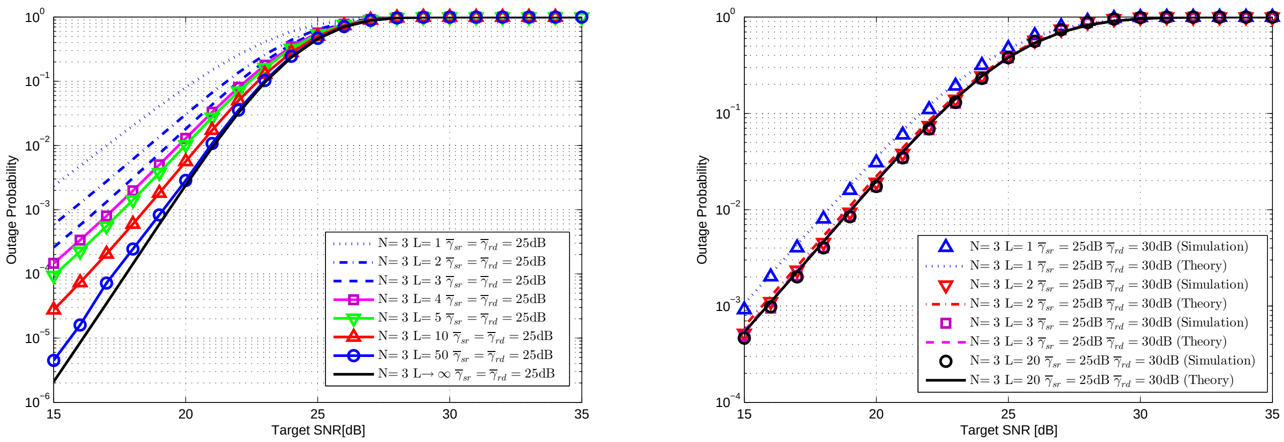

(a) Symmetric channels (b) Asymmetric channels

Fig. 4. Outage probability performance of the max-link scheme for different buffer length L.

Fig. 5 shows how the outage performance changes with different relay numbers N for a fixed buffer size $L = 8$, where the asymmetric channel configuration with $\bar{\gamma}_{sr} = 30$dB and $\bar{\gamma}_{rd} = 25$dB is considered. It is clearly shown that the outage performance improves with more relays. The results for other channel configurations are similar so they are not presented.

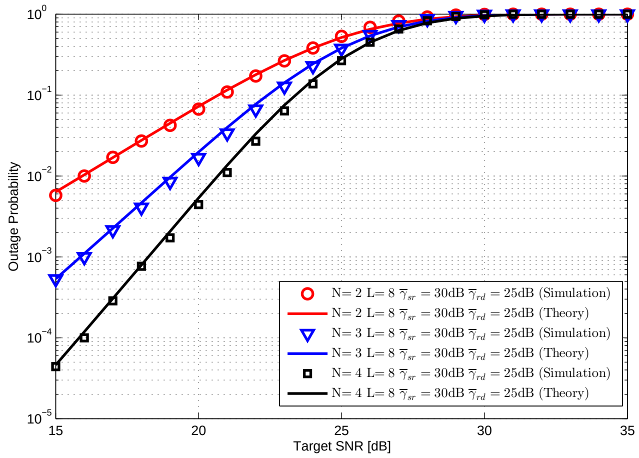

Fig. 5. Outage probability performance of the max-link scheme for different relay number N.

B. Outage performance comparison between of the AF max-link and max-SNR schemes

Fig. 6 compares the proposed AF max-link and traditional max-SNR schemes in symmetric and asymmetric channels. For fair comparison, we let $\bar{\gamma}_{sr}(\text{dB}) + \bar{\gamma}_{rd}(\text{dB}) = 40\text{dB}$ in all cases. It is clearly shown that, for the both the AF max-link and max-SNR schemes, the best outage performance is achieved in the symmetric channel. Moreover, the outage performance advantage of the AF max-link scheme over the traditional max-SNR scheme is also more significant in the symmetric than in the asymmetric channels. For example, when the target SNR=10dB, the outage probability difference between the max-link and max-SNR are approximately as large as 28dB for symmetric channels, and only about 2dB for asymmetric channels[6].

This can be explained as following: In the AF max-link scheme, as is shown in (10), the outage performance depends on both the outage probability for every buffer state and the distributions of the buffer states, because different buffer state may correspond to different available links for the relay selection. On the one hand, the outage probability for a given buffer state is always minimized in the symmetric channel. This is because that, as is shown in the outage bound in Section V-A, the outage probability for any buffer state depends on the minimum SNR of the source-to-relay and relay-to-destination channels, which is clearly minimized in the symmetric channels. On the other hand, if the channels become more asymmetric, the relay buffers are more likely to be full or empty, corresponding to fewer available links, which also deteriorates the outage performance.

[6]Outage probability in dB = 10 log(outage probability)

In comparison, the traditional AF max-SNR scheme does not have buffer states and the available links for selection is always equal to the relay numbers. Thus the outage performance solely depends on the minimum SNR of the source-to-relay and relay-to-destination channels, and is optimum in symmetric channels. Therefore, when the channels become more asymmetric, there are two and one deteriorating factors in the outage performance for the max-link and max-SNR respectively, so that the outage performance of the max-link deteriorates faster than that of the max-SNR scheme. Therefore, compared with the traditional relay selection scheme, the buffer-aided max-link scheme is most effective in the symmetric channel configuration.

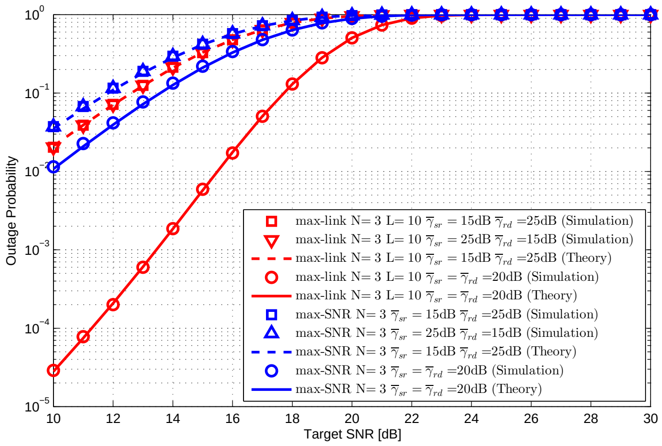

Fig. 6. Outage performance comparison between the AF max-link and max-SNR schemes with different channel configurations.

C. Diversity order and coding gain

In order to show the diversity gain, Fig. 7 considers a symmetric channel configuration that $\bar{\gamma}_{sr} = \bar{\gamma}_{rd} = 25$dB. As is proved in Section V, the diversity orders of the AF max-link scheme are N and $2N$, when the buffer sizes are $L = 1$ and $L \to \infty$ respectively. On the other hand, diversity order of the max-SNR is N. Therefore, the max-link schemes with $(N, L = 1)$ and $(N, L \to \infty)$ have the same diversity orders as those for the max-SNR with N and $2N$ respectively, which is clearly verified in Fig. 7.

It is interesting to observe that, because of the coding gain, the max-link scheme with $(N = 5, L = 1)$ has significant better outage performance than the max-SNR scheme with $N = 5$, though they have the same diversity orders. Fig. 7 shows that, when $\mathrm{SNR} = 14$dB, the outage probability difference between max-SNR with $N = 5$ and max-link with $(N = 5, L = 1)$ is approximately 11dB, which well matches the approximate coding gain obtained from (67) that $10(N-1)\log 2 = 12$dB when $N = 5$.

On the other hand, for the max-link scheme $N = 5, L \to \infty$, the available link for every buffer state is $2N = 10$. Then following the similar procedure in Section V, we can obtain that the coding gain of the max-link with $N = 5, L \to \infty$ over the max-SNR with $2N = 10$ is approximately $10(2N-1)\log 2 =$ 27dB. But Fig. 7 shows that, when $\mathrm{SNR} = 14$dB, the outage probability difference between the max-SNR with $N = 10$ and max-link with ($N = 5, L \to \infty$) is approximately 31dB, which well matches the analytical result.

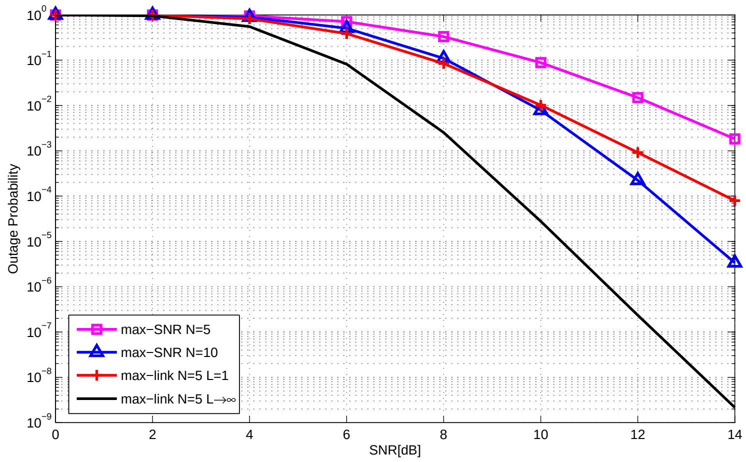

Fig. 7. Diversity order and coding gain of the AF max-link scheme.

VIII. CONCLUSION

In this paper, we carefully studied the performance of buffer-aided AF max-link relay selection scheme for both symmetric and asymmetric channels. We derive the closed form expression of the outage probability of the proposed scheme. The results showed that the max-link scheme is most effective over the traditional max-SNR scheme when the source-to-relay and relay-to-destination links are symmetric. We also derived the average packet delay of the max-link scheme under both both symmetric and asymmetric channel configurations. We proved that the diversity order of the AF max-link scheme is between N and $2N$, where the lower and upper limits were obtained when the buffer size is 1 and ∞ respectively. We also analytically showed the coding gain of the max-link scheme over the traditional max-SNR scheme. Finally, extensive numerical simulations were given to verify the analysis in this paper.

APPENDIX - PROOF OF (15)

Since the integration area of (14) is closed by the curve $\frac{\gamma_{th}(x+1)}{x-\gamma_{th}}$, $x \geq 0$ axis and $y \geq 0$ axis, the integration can be split into three parts as

$$\begin{aligned} P(\gamma_D^{(s_i,s_j)} \leq \gamma_{th}) &= \underbrace{\int_{\gamma_{th}}^{\infty} \int_{0}^{\gamma_{th}} f_{\gamma_{SR_k}^{(s_i)} \gamma_{R_kD}^{(s_j)}}(x,y)\, dx\, dy}_{A} + \underbrace{\int_{0}^{\gamma_{th}} \int_{0}^{\infty} f_{\gamma_{SR_k}^{(s_i)} \gamma_{R_kD}^{(s_j)}}(x,y)\, dx\, dy}_{B} \\ &+ \underbrace{\int_{\gamma_{th}}^{\infty} \int_{\gamma_{th}}^{\frac{\gamma_{th}(y+1)}{y-\gamma_{th}}} f_{\gamma_{SR_k}^{(s_i)} \gamma_{R_kD}^{(s_j)}}(x,y)\, dx\, dy}_{C} . \end{aligned} \tag{68}$$

Parts A and B can be obtained as

$$\begin{aligned} A &= \int_{\gamma_{th}}^{\infty} \int_{0}^{\gamma_{th}} f_{\gamma_{SR_k}^{(s_i)} \gamma_{R_kD}^{(s_j)}}(x,y)\, dx\, dy \\ &= [1 - F_{\gamma_{R_kD}^{(s_j)}}(\gamma_{th})] F_{\gamma_{SR_k}^{(s_i)}}(\gamma_{th}) \\ B &= \int_{0}^{\gamma_{th}} \int_{0}^{\infty} f_{\gamma_{SR_k}^{(s_i)} \gamma_{R_kD}^{(s_j)}}(x,y)\, dx\, dy \\ &= F_{\gamma_{R_kD}^{(s_j)}}(\gamma_{th}), \end{aligned} \tag{69}$$

respectively. Part C is further divided into parts C_1 and C_2 as

$$\begin{aligned} C &= \int_{\gamma_{th}}^{\infty} f_{\gamma_{R_kD}^{(s_j)}}(y) \int_{\gamma_{th}}^{\frac{\gamma_{th}(y+1)}{y-\gamma_{th}}} f_{\gamma_{SR_k}^{(s_i)}}(x)\, dx\, dy \\ &= \underbrace{\int_{\gamma_{th}}^{\infty} f_{\gamma_{R_kD}^{(s_j)}}(y) F_{\gamma_{SR_k}^{(s_i)}}[\frac{\gamma_{th}(y+1)}{y-\gamma_{th}}]\, dy}_{C_1} - \underbrace{[1 - F_{\gamma_{R_kD}^{(s_j)}}(\gamma_{th})] F_{\gamma_{SR_k}^{(s_i)}}(\gamma_{th})}_{C_2} . \end{aligned} \tag{70}$$

Noticing C_2 is equal to part A, we now need to calculate part C_1. First applying a binomial expansion on $F_{\gamma_{SR_k}^{(s_i)}}[\frac{\gamma_{th}(y+1)}{y-\gamma_{th}}]$ which gives

$$\begin{aligned} F_{\gamma_{SR_k}^{(s_i)}}[\frac{\gamma_{th}(y+1)}{y-\gamma_{th}}] &= \sum_{m=0}^{K_{sr}^{(s_i)}} \sum_{n=0}^{K_{rd}^{(s_i)}} C_{K_{sr}^{(s_i)}}^{m} C_{K_{rd}^{(s_i)}}^{n} (-1)^{m+n} e^{-\frac{m}{\bar{\gamma}_{sr}} \cdot \frac{\gamma_{th}(y+1)}{y-\gamma_{th}}} e^{-\frac{n}{\bar{\gamma}_{rd}} \cdot \frac{\gamma_{th}(y+1)}{y-\gamma_{th}}} \\ &= \underset{(m,n)=(0,0)}{1} + \sum_{\substack{m=0 \\ (m,n)\neq(0,0)}}^{K_{sr}^{(s_i)}} \sum_{n=0}^{K_{rd}^{(s_i)}} C_{K_{sr}^{(s_i)}}^{m} C_{K_{rd}^{(s_i)}}^{n} (-1)^{m+n} e^{-(\frac{m}{\bar{\gamma}_{sr}} + \frac{n}{\bar{\gamma}_{rd}}) \cdot \frac{\gamma_{th}(y+1)}{y-\gamma_{th}}} . \end{aligned} \tag{71}$$

We let $M_4 = \frac{m}{\bar{\gamma}_{sr}} + \frac{n}{\bar{\gamma}_{rd}}$ and substituting (71) into part C_1 gives

$$\begin{aligned} C_1 &= \int_{\gamma_{th}}^{\infty} f_{\gamma_{R_kD}^{(s_j)}}(y)\,dy + \sum_{\substack{m=0\\(m,n)\neq(0,0)}}^{K_{sr}^{(s_i)}} \sum_{n=0}^{K_{rd}^{(s_i)}} C_{K_{sr}^{(s_i)}}^{m} C_{K_{rd}^{(s_i)}}^{n} (-1)^{m+n} \int_{\gamma_{th}}^{\infty} f_{\gamma_{R_kD}^{(s_j)}}(y) e^{-M_4\cdot\frac{\gamma_{th}(y+1)}{y-\gamma_{th}}}\,dy \\ &= \underbrace{[1 - F_{\gamma_{R_kD}^{(s_j)}}(\gamma_{th})]}_{C_{11}} + \underbrace{\sum_{\substack{m=0\\(m,n)\neq(0,0)}}^{K_{sr}^{(s_i)}} \sum_{n=0}^{K_{rd}^{(s_i)}} C_{K_{sr}^{(s_i)}}^{m} C_{K_{rd}^{(s_i)}}^{n} (-1)^{m+n} \int_{\gamma_{th}}^{\infty} f_{\gamma_{R_kD}^{(s_j)}}(y) e^{-M_4\cdot\frac{\gamma_{th}(y+1)}{y-\gamma_{th}}}\,dy,}_{C_{12}} \end{aligned} \tag{72}$$

which is further split into another two parts as C_{11} (for $(m,n) = (0,0)$) and C_{12} (for $(m,n) \neq (0,0)$) respectively. Noticing C_{11} is actually equal to $1 - B$ as is shown in (69).

Applying a binomial expansion on $f_{\gamma_{R_kD}^{(s_j)}}(y)$ which gives

$$\begin{aligned} f_{\gamma_{R_kD}^{(s_j)}}(y) = &\sum_{a_1=0}^{K_{sr}^{(s_j)}-1} \sum_{a_2=0}^{K_{rd}^{(s_j)}} C_{K_{sr}^{(s_j)}-1}^{a_1} C_{K_{rd}^{(s_j)}}^{a_2} (-1)^{a_1+a_2} \frac{K_{sr}^{(s_j)}}{\bar{\gamma}_{sr}} e^{-M_1 y} \\ &+ \sum_{a_3=0}^{K_{rd}^{(s_j)}-1} \sum_{a_4=0}^{K_{sr}^{(s_j)}} C_{K_{rd}^{(s_j)}-1}^{a_3} C_{K_{sr}^{(s_j)}}^{a_4} (-1)^{a_3+a_4} \frac{K_{rd}^{(s_j)}}{\bar{\gamma}_{rd}} e^{-M_2 y} \end{aligned} \tag{73}$$

where $M_1 = \frac{1}{\bar{\gamma}_{sr}} + \frac{a_1}{\bar{\gamma}_{sr}} + \frac{a_2}{\bar{\gamma}_{rd}}$ and $M_2 = \frac{1}{\bar{\gamma}_{rd}} + \frac{a_3}{\bar{\gamma}_{rd}} + \frac{a_4}{\bar{\gamma}_{sr}}$. Thus for C_{12},

$$\begin{aligned} C_{12} =& \sum_{\substack{m=0\\(m,n)\neq(0,0)}}^{K_{sr}^{(s_i)}} \sum_{n=0}^{K_{rd}^{(s_i)}} C_{K_{sr}^{(s_i)}}^{m} C_{K_{rd}^{(s_i)}}^{n} (-1)^{m+n} \cdot \\ & [\sum_{a_1=0}^{K_{sr}^{(s_j)}-1} \sum_{a_2=0}^{K_{rd}^{(s_j)}} C_{K_{sr}^{(s_j)}-1}^{a_1} C_{K_{rd}^{(s_j)}}^{a_2} (-1)^{a_1+a_2} \frac{K_{sr}^{(s_j)}}{\bar{\gamma}_{sr}} \int_{\gamma_{th}}^{\infty} e^{-M_1 y} e^{-M_4\cdot\frac{\gamma_{th}(y+1)}{y-\gamma_{th}}}\,dy \\ & + \sum_{a_3=0}^{K_{rd}^{(s_j)}-1} \sum_{a_4=0}^{K_{sr}^{(s_j)}} C_{K_2^{rd}-1}^{a_3} C_{K_{sr}^{(s_j)}}^{a_4} (-1)^{a_3+a_4} \frac{K_{rd}^{(s_j)}}{\bar{\gamma}_{rd}} \int_{\gamma_{th}}^{\infty} e^{-M_2 y} e^{-M_4\cdot\frac{\gamma_{th}(y+1)}{y-\gamma_{th}}}\,dy] \\ =& \sum_{\substack{m\\(m,n)\neq(0,0)}}^{K_{sr}^{(s_i)}} \sum_{n}^{K_{rd}^{(s_i)}} C_{K_{sr}^{(s_i)}}^{m} C_{K_{rd}^{(s_i)}}^{n} (-1)^{m+n} 2 e^{-M_4\gamma_{th}} \sqrt{M_4 M_{\gamma_{th}}} \cdot \\ & \cdot [\frac{K_{sr}^{(s_j)}}{\bar{\gamma}_{sr}} \sum_{a_1=0}^{K_{sr}^{(s_j)}-1} \sum_{a_2=0}^{K_{rd}^{(s_j)}} (-1)^{a_1+a_2} C_{K_{sr}^{(s_j)}-1}^{a_1} C_{K_{rd}^{(s_j)}}^{a_2} \frac{e^{-M_1\gamma_{th}}}{\sqrt{M_1}} \mathcal{B}(1, 2\sqrt{M_1 M_4 M_{\gamma_{th}}}) \\ & + \frac{K_{rd}^{(s_j)}}{\bar{\gamma}_{rd}} \sum_{a_3=0}^{K_{rd}^{(s_j)}-1} \sum_{a_4=0}^{K_{sr}^{(s_j)}} (-1)^{a_3+a_4} C_{K_{rd}^{(s_j)}-1}^{a_3} C_{K_{sr}^{(s_j)}}^{a_4} \frac{e^{-M_2\gamma_{th}}}{\sqrt{M_2}} \mathcal{B}(1, 2\sqrt{M_2 M_4 M_{\gamma_{th}}})] \end{aligned} \tag{74}$$

where $M_{\gamma_{th}} = \gamma_{th}(\gamma_{th}+1)$ and $\mathcal{B}$ denotes the modified Bessel function of the second kind [15]. Finally, substituting A, B and C back into (70) gives

$$
\begin{aligned}
P(\gamma_D^{(s_i,s_j)} < \gamma_{th}) = 1 + &\sum_{\substack{m \\ (m,n)\neq(0,0)}}^{K_{sr}^{(s_i)}} \sum_{n}^{K_{rd}^{(s_i)}} C_{K_{sr}^{(s_i)}}^{m} C_{K_{rd}^{(s_i)}}^{n} (-1)^{m+n} 2e^{-M_4\gamma_{th}} \sqrt{M_4 M_{\gamma_{th}}} \cdot \\
&\cdot \Big[\frac{K_{sr}^{(s_j)}}{\bar{\gamma}_{sr}} \sum_{a_1=0}^{K_{sr}^{(s_j)}-1} \sum_{a_2=0}^{K_{rd}^{(s_j)}} (-1)^{a_1+a_2} C_{K_{sr}^{(s_j)}-1}^{a_1} C_{K_{rd}^{(s_j)}}^{a_2} \frac{e^{-M_1\gamma_{th}}}{\sqrt{M_1}} \mathcal{B}(1, 2\sqrt{M_1 M_4 M_{\gamma_{th}}}) \\
&+ \frac{K_{rd}^{(s_j)}}{\bar{\gamma}_{rd}} \sum_{a_3=0}^{K_{rd}^{(s_j)}-1} \sum_{a_4=0}^{K_{sr}^{(s_j)}} (-1)^{a_3+a_4} C_{K_{rd}^{(s_j)}-1}^{a_3} C_{K_{sr}^{(s_j)}}^{a_4} \frac{e^{-M_2\gamma_{th}}}{\sqrt{M_2}} \mathcal{B}(1, 2\sqrt{M_2 M_4 M_{\gamma_{th}}}) \Big]
\end{aligned}
\tag{75}
$$

■

REFERENCES

[1] W. Su and X. Liu, "On optimum selection relaying protocols in cooperative wireless networks," *IEEE Trans. Wireless Commun.*, vol. 58, pp. 52–57, Jan. 2010.

[2] A. Bletsas, A. Khisti, D. P. Reed, and A. Lippman, "A simple cooperative diversity method based on network path selection," *IEEE J. Sel. Areas Commun.*, vol. 24, pp. 659–672, March 2006.

[3] A. Ikhlef, D. S. Michalopoulos, and R. Schober, "Buffers improve the performance of relay selection," *in Proc. 2011 IEEE Global Commun. Conf, Houston,Texas,USA*, pp. 1–6, Dec. 2011.

[4] I. Krikidis, T. Charalambous, and J. S. Thompson, "Buffer-aided relay selection for cooperative diversity systems without delay constraints," *IEEE Trans. Wireless Commun.*, vol. 11, no. 5, pp. 1957–1967, May 2012.

[5] H. Liu, P. Popovski, E. Carvalho, and Y. Zhao, "Sum-rate optimization in a two-way relay network with buffering," *IEEE Commun. Letters*, vol. 17, pp. 95–98, Jan. 2013.

[6] A. Ikhlef, D. S. Michalopoulos, and R. Schober, "Max-max relay selection for relays with buffers," *IEEE Trans. Wireless Commun.*, vol. 11, no. 3, pp. 1124–1135, May 2012.

[7] N. Zlatanov, R. Schober, and L. Lampe, "Buffer-aided relaying in a three node network," *in Proc. 2012 IEEE International Symposium on Information Theory Proceedings,Cambridge,Massachusetts,USA*, pp. 781–785, July 2012.

[8] N. Zlatanov, R. Schober, and P. Popovski, "Buffer-aided relaying with adaptive link selection," *IEEE J. Sel. Areas Commun.*, vol. 31, pp. 1–13, Oct. 2012.

[9] B. Barua, H. Q. Ngo, and H. Shin, "On the sep of cooperative diversity with opportunistic relaying," *IEEE Commun. Letters*, vol. 12, pp. 727–729, Oct. 2008.

[10] I. Krikidis, J. S. Thompson, S. McLaughlin, and N. Goertz, "Amplify-and-forward with partial relay selection," *IEEE Commun. Letters*, vol. 12, pp. 235–237, Apr. 2008.

[11] H. A. Suraweera, M. Soysa, C. Tellambura, and H. K. Garg, "Performance analysis of partial relay selection with feed back delay," *IEEE Signal Process. Lett*, vol. 17, pp. 531–534, June 2010.

[12] W. J. Huang, Y. W. Hong, and C. C. J. Kuo, "Lifetime maximization for amplify-and-forward cooperative networks," *IEEE Trans. Wireless Commun.*, vol. 7, pp. 1800–1805, May 2008.

[13] I. Krikidis, J. S. Thompson, S. McLaughlin, and N. Goertz, “Max-min relay selection for legacy amplify-and-forward systems with interference,” *IEEE Trans. Wireless Commun.*, vol. 8, pp. 3016–3027, June 2009.

[14] H. A. David, “Order statistics second edition,” *John Wiley Sons Ltd*, 1981.

[15] M. Abramowitz and I. A. Stegun, “Handbook of mathematical functions: with formulas, graphs, and mathematical tables,” *New York: Dover*, 1965.

[16] C. M. Grinstead and J. L. Snell, “Introduction to probability: Second revised edition,” *American Mathematical Society*, 1991.

[17] J. R. Norris, “Markov chains,” *Cambridge University Press*, 1998.

[18] A. Berman and R. J. Plemmons, “Nonnegative matrices in the mathematical sciences,” *Society of industrial and applied mathematics*, 1994.

[19] J. N. Laneman, D. N. C. Tse, and G. W. Wornell, “Cooperative diversity in wireless networks: Efficient protocols and outage behavior,” *IEEE Trans. Inform. Theory*, vol. 50, pp. 3062–3080, Dec. 2004.